plexes of both the Schiff bases II and III in the aminobenzyl alcohol or aminophenol part of the molecules. The CH_2 groups are very close to the bridging enolic oxygen atoms in the oxovanadium(IV) complexes of II but are far away from the bridging phenolic oxygen atoms in the oxovanadium(IV) complexes of III. The presence of the CH_2 groups close to the bridging oxygen atoms in the oxovanadium(IV) complexes of II would lead to a longer V–V distance due to steric influence; hence the magnetic interaction will be weaker in oxovanadium(IV) complexes of II than in those of III. Furthermore, the delocalization of the vanadium(IV) electrons will be more effective in complexes of III in comparison to the complexes of II due to the difference in position of the CH_2 group. The magnetic data of the oxovanadium(IV) complexes of II and III preclude the possibility of bridging through the phenolic oxygen atoms of salicylaldehyde part of the molecule. If phenolic oxygen atoms of the salicylaldehyde moiety are involved in the bridging, then J should not vary in these two series of complexes since the electronic environment in the chelate ring is the same. In oxovanadium(IV) complexes of IV ($n = 2$), the magnetic exchange interaction has been found

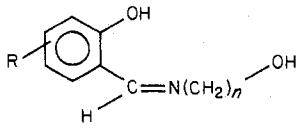

IV: $n = 2$ or 3

to be of greater magnitude than in the oxovanadium(IV) complexes of IV ($n = 3$).[17] This has been explained on the basis of the chelate ring effect; the magnetic interaction is greater in the case of a five-membered chelate ring ($n = 2$ complexes) than in the case of a six-membered chelate ring ($n = 3$ complexes) in the amino alcohol part of the molecules. As the oxovanadium(IV) complex of III has greater magnetic-exchange interaction than that of I, it is apparent that the chelate ring effect is not operative in these systems with more aromatic character and more steric rigidity (cf. less aromatic character and less steric rigidity in oxovanadium(IV) complexes of IV).

Acknowledgment. The authors are indebted to the Department of Atomic Energy (Government of India), CSIR (India), and the faculty research fund of the Regional Engineering College, Kurukshetra, for financial support. They thank Dr. S. Banerjee for experimental assistance.

Registry No. VO(sal-*o*-hydroxybenzylamine), 69204-55-3; VO(5-chlorosal-*o*-hydroxybenzylamine), 69204-54-2; VO(5-bromosal-*o*-hydroxybenzylamine), 69204-53-1; VO(4-methoxysal-*o*-hydroxybenzylamine), 69204-52-0; VO(3,5-dichlorosal-*o*-hydroxybenzylamine), 69204-51-9; VO(hydrox-*o*-hydroxybenzylamine), 69204-50-8; sal, 90-02-8; 5-chlorosal, 635-93-8; 5-bromosal, 1761-61-1; 4-methoxysal, 673-22-3; 3,5-dichlorosal, 90-60-8; hydrox, 708-06-5; *o*-hydroxybenzylamine, 932-30-9; oxovanadium(IV) dichloride, 10213-09-9.

References and Notes

(1) W. E. Hatfield and R. Whyman, *Transition Met. Chem.*, **5**, 47 (1969).
(2) J. A. Bertrand, J. L. Breece, A. R. Kalyanaraman, G. J. Long, and W. A. Baker, Jr., *J. Am. Chem. Soc.*, **92**, 5233 (1970).
(3) J. A. Bertrand and P. G. Eller, *Inorg. Chem.*, **13**, 928 (1974).
(4) D. J. Hodgson, *Prog. Inorg. Chem.*, **19**, 173 (1975).
(5) A. P. Ginsberg, E. Koubeck and H. J. Williams, *Inorg. Chem.*, **5**, 1656 (1966).
(6) A. Syamal and K. S. Kale, *J. Indian Chem. Soc.*, in press.
(7) F. J. Welcher, "Organic Analytical Reagents", Vol. III, D. Van Nostrand Co., New York, 1947, p 254.
(8) L. C. Raiford and E. P. Clark, *J. Am. Chem. Soc.*, **45**, 1738 (1923).
(9) B. N. Figgis and R. S. Nyholm, *J. Chem. Soc.*, 381 (1959).
(10) B. N. Figgis and J. Lewis, "Modern Coordination Chemistry", J. Lewis and R. G. Wilkins, Eds., Interscience, New York, 1960, p 403.
(11) B. Bleaney and K. D. Bowers, *Proc. R Soc. London, Ser. A*, **214**, 451 (1952).
(12) J. Selbin, *Chem. Rev.*, **65**, 293 (1966); *Coord. Chem. Rev.*, **1**, 293 (1966).
(13) M. Mathew, A. J. Carty, and G. J. Palenik, *J. Am. Chem. Soc.*, **92**, 3197 (1970).
(14) E. Sinn and C. M. Harris, *Coord. Chem. Rev.*, **4**, 391 (1969); T. Tokii, Y. Muto, M. Kato, and H. B. Jonassen, *J. Inorg. Nucl. Chem.*, **34**, 3377 (1972).
(15) B. N. Figgis, "Introduction to Ligand Fields", Wiley, New York, 1966, p 266.
(16) A. Syamal, *Coord. Chem. Rev.*, **16**, 309 (1975).
(17) A. Syamal, E. F. Carey, and L. J. Theriot, *Inorg. Chem.*, **12**, 245 (1973).

Contribution from the Center for Surface and Coatings Research, Sinclair Laboratory, Lehigh University, Bethlehem, Pennsylvania 18015

Electron Paramagnetic Resonance Investigation of Copper(II) Complexes with Reversed g Values in A and Y Zeolites

RICHARD G. HERMAN

Received September 25, 1978

The electron paramagnetic resonance (EPR) spectra of evacuated low ion exchanged copper(II) Y and A zeolites are presented, in which reversed g values are observed. The EPR parameters for CuY-10 and CuA-6 are $g_\perp = 2.32$ with $g_\parallel = 2.00$ (102) and $g_\perp = 2.30$ with $g_\parallel = 1.99$ (85), respectively, where the numbers in parentheses are the hyperfine splitting values (in gauss). It is proposed that these reversed spectra are due to pentacoordinated copper(II) ions held in the trigonal sodalite cage windows with water molecules in the axial positions to yield trigonal-bipyramidal complexes. Using a reoxidation technique, a similar diammine complex has been formed, which has EPR parameters of $g_\perp = 2.32$ and $g_\parallel = 1.97$ (131). The latter values are similar to those previously reported for an amminecopper(II) complex formed by an evacuation procedure. Only part of the divalent copper in the zeolites form the bipyramidal complexes that are decomposed by thermal treatments.

Introduction

Synthetic zeolites, such as A, L, X, and Y, have rigid three-dimensional lattices that provide interesting media in which to study the coordination chemistry of transition-metal ions. The exchangeable cations can be located in a number of coordination sites in the dehydrated zeolites, where they are usually coordinatively unsaturated. This results in the ready reactivity of the cations toward a wide range of ligands (L) to form complexes ranging from lattice-held ML to free ML_6 complexes located in the supercages.

Zeolite A is structurally fairly simple and the cation-exchanged forms of this zeolite have been the most extensively

0020-1669/79/1318-0995$01.00/0 © 1979 American Chemical Society

characterized by X-ray diffraction techniques. By structural determination, it has been found that in hydrated A zeolites, Ni(II),[1] Co(II),[2] and Zn(II)[3] ions are tetrahedrally coordinated (except one cation in each case, which is found in the center of the sodalite cage) and are located in the 6-ring windows[4] with a water molecule at one apex. In contrast, all Mn(II) ions in the A zeolite were found in the 6-ring site but coordinated to two water molecules to form a trigonal-bipyramidal complex.[5] Unfortunately, the hydrated Cu(II) A structure has not yet been solved by crystallographic methods. Prior to the structural work, the same conclusions were reached in regard to the coordination spheres of Ni(II)[6] and Co(II)[7] in partially ion exchanged, partially dehydrated A zeolites by utilizing optical reflectance spectroscopy. The symmetry of the latter lattice-held complexes is distinctly C_{3v}. Little research has been carried out optically on hydrated Cu(II) A, but it has been reported that the optical spectrum of dehydrated Cu(II) A is identical with that of activated copper(II) Y zeolite.[8]

Zeolite Y consists of the supercages and sodalite cages found in A zeolite (plus connecting hexagonal prisms) and can stabilize similar transition-metal complexes. No *single-crystal* structural determinations have been carried out with the transition metal ion exchanged Y zeolites, and few optical reflectance investigations have been reported on these systems. In hydrated copper(II) Y zeolites, the absorption band located near 800 nm is rather broad. Upon dehydration, the band is moved toward longer wavelengths[8,9] and appears to consist of a number of components. Although an attempt has been made to assign the components to a number of copper(II) ions with various degrees of hydration, e.g., $Cu(H_2O)_4^{2+}$, $Cu(H_2O)_1^{2+}$, $Cu(H_2O)_6^{2+}$, and lattice-held Cu(II),[9] the components (shoulders) might be d–d transitions, of which there could be two or three per nonequivalent copper ion. Thus, in the dehydrated and partially dehydrated samples with two or three nonequivalent Cu(II) ions,[10] there could be up to nine components under the absorption band envelope.

The copper Y zeolites are more readily examined by electron paramagnetic resonance (EPR) techniques. During the evacuation of a hydrated copper(II) Y zeolite, the appearance of a reversed EPR spectrum ($g_\perp > g_\parallel$) was noted, and this was attributed to a mono- or diaquocopper(II) complex.[10] Analogous to this, a reversed spectrum was obtained by evacuation (at 373 K) of ammonia-saturated copper(II) Y zeolites.[11-13] The reversed spectrum, with $g_\parallel = 2.02 \pm 0.01$ and $g_\perp = 2.25 \pm 0.01$,[11,12] was assigned to a monoammine-copper(II) complex with distorted tetrahedral symmetry. However, volumetric desorption experiments indicated the ammonia to copper ratio to be 1.5,[12] 1.76,[14] and 1.52[14] for various CuY zeolites when the desorption temperature was about 295 K. Since a Cu(II) ion in a compressed tetrahedral configuration (D_{2d}) should have its unpaired d electron in the d_{xy} or $d_{x^2-y^2}$ orbital and would be expected to generate a "normal" EPR spectrum, the present study was undertaken to reinvestigate the aquo and ammine complexes that form upon evacuation of the designated copper(II) Y zeolites, to report the EPR parameters of the probable $(O(2))_3Cu(H_2O)_2^{2+}$ complex (where O(2) represents a lattice oxygen in the 6-ring window), and to clarify the symmetry considerations of these complexes.

Experimental Section

Materials. The copper(II) exchanged A and Y zeolites were prepared by continuously stirring the zeolites at ambient temperature for 4 h in filtered $Cu(NO_3)_2 \cdot 3H_2O$ solutions (volume to mass ratio = 20 cm^3/g). The zeolites were then filtered, washed with ten portions of water (a total of approximately 100 mL was used), and air-dried. The lattice-held copper(II) and sodium(I) concentrations were determined by atomic absorption following the back-exchange with silver ion. The compositions of the CuY zeolites are given elsewhere.[10] The copper A zeolites used in this investigation were CuA-3 and CuA-6, where the figure shows the exchange level of Cu(II) in percent of the total cation exchange capacity.

The ultrahigh-purity grade gases were obtained from Air Products and Chemicals, Inc. Water that was utilized in the readsorption experiments was repeatedly purified by the freeze–thaw evacuation technique.

Sample Treatments. For the preparation of $Cu(H_2O)_n^{2+}$ complexes, where $n < 4$, the zeolites were placed in a conventional EPR batch sample cell (cell volume to zeolite mass ratio was ≈200 cm^3/g) having a 4-mm o.d. quartz side arm that could be inserted into an EPR microwave cavity. The cell was then evacuated dynamically at 10^{-4} torr (1 torr = 133.3 N/m^2) at ambient temperature, and periodically an EPR spectrum was obtained. Subsequently, the CuY-10 sample was activated to 773 K using 1-h, 100 K increments, and water vapor was added to the sample cell at ambient temperature in small "slugs".

The $Cu(NH_3)_n^{2+}$ complexes, where $n < 4$, were prepared by two procedures. Portions of CuY-10 and CuY-32 were dehydrated to 673 K using the above described stepwise procedure after evacuating the cell for 0.5 h at ambient temperature. Excess ammonia was then added and EPR spectra of the resultant samples were recorded. Evacuation was then carried out at 373 K for various lengths of time and EPR spectra were obtained.

A CuY-60 sample (0.100 g) was evacuated for 0.5 h, dehydrated to 773 K using the stepwise procedure, and then reduced repeatedly with CO at 773 K until complete extinction of the Cu(II) EPR signal was achieved. Excess NH_3 was added and after equilibration for 1 h, evacuation was carried out for 0.5 h at 10^{-4} torr. To the sample was added 20 Torr of NO, and EPR spectra were obtained after various equilibration times.

A fresh portion of CuY-60 was dehydrated and reduced as described above. Excess NH_3 was added to the sample, and after 1 h the ammonia was expanded out of the cell until an equilibrium pressure of 2 torr was obtained. After cooling of the sample to approximately 200 K, 10 torr of O_2 was added and EPR spectra were obtained following various periods of equilibration.

EPR Spectroscopy. EPR spectra were recorded at 77 K in the X-band region with a Varian E-6S spectrometer equipped with a TE_{102} mode cavity. A phosphorus-doped silicon standard or a sample of pitch in KCl was used as a reference standard for g-value determinations.

Results

Copper(II) Aquo Complexes. The initial hydrated CuY zeolites contained about 260 water molecules per unit cell, and the EPR spectrum for hydrated CuY-10 is shown in Figure 1A. The EPR parameters are $g_\parallel = 2.389$ (125) and $g_\perp = 2.053$, where the number in parentheses is the hyperfine splitting value in units of gauss, and these correspond to the hexaaquocopper(II) complex held in the supercages of the Y zeolite structure.[10] During the first 0.5 h of evacuation, it appeared that much of the water was removed from the zeolite, and after 18 h of evacuation two distinct sets of EPR parameters were evident (Figure 1B). These two sets consisted of $g_\parallel^1 = 2.365$ (121), $g_\perp^1 = 2.063$ (18), $g_\parallel^2 = 2.313$ (162), and $g_\perp^2 = 2.026$. Very small high-field lines were just becoming observable, but after 87 h of evacuation they were quite clear. In addition, Figure 1C shows that a line has appeared in the area of $g = 2.3$. These lines are due to the newly formed copper(II) aquo complex and yield $g_\parallel^4 = 2.00$ (102) and $g_\perp^4 = 2.32$. This complex is destroyed by heating the zeolite at 373 K for 1 h under a dynamic vacuum, as shown in Figure 1D, and the sample turned from light blue to light green. Following dehydration to 773 K, reoxidation by 50 torr of O_2 at the same temperature for 0.25 h, and evacuation for 12 h, water vapor was added to the zeolite. The EPR spectrum reverted to that of the hexaaquocopper(II) species; see Figure 1A. Subsequent evacuation led to the same series of observations as described above, with the high-field lines becoming evident after 46 h of evacuation.

Evacuation of a CuY-2 zeolite did not produce the high-field lines within 200 h, although the initial spectrum corresponded to the $Cu(H_2O)_6^{2+}$ complex. Upon evacuation of CuY-60 for

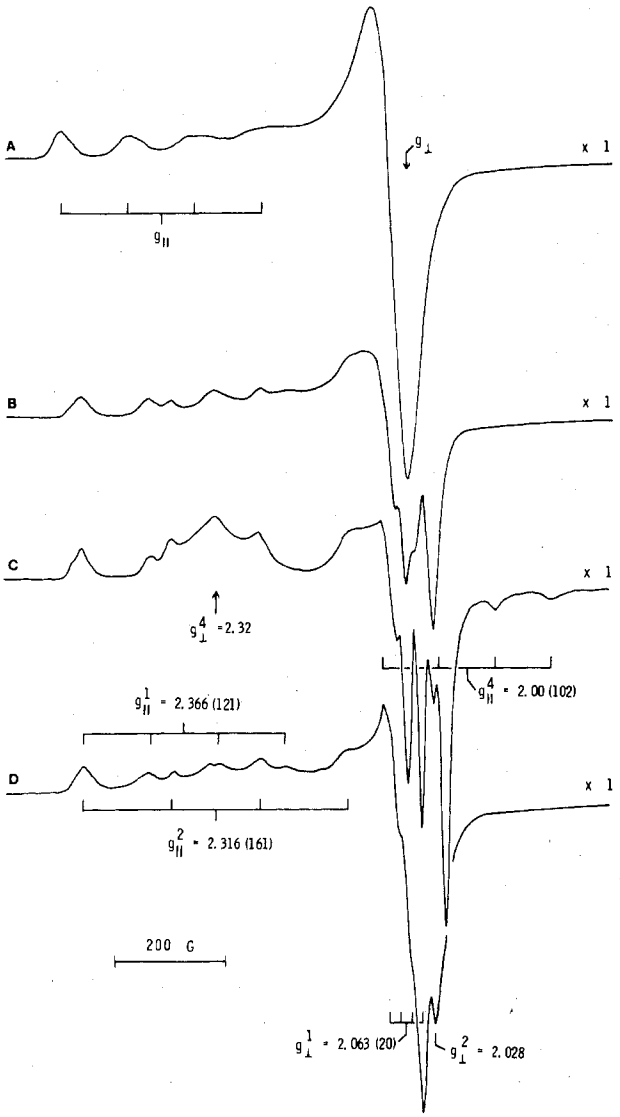

Figure 1. EPR spectra obtained for a sample of hydrated CuY-10 that was evacuated at ambient temperature using a dynamic vacuum for (A) 0 h, for (B) 18 h, and for (C) 87 h. Subsequent evacuation at 373 K for 1 h yielded spectrum D.

up to 400 h, no evidence for the presence of the high-field set of lines was found.

A CuA-3 zeolite was evacuated at ambient temperature in a series of steps for a total of 85 h. It appeared that an aquo complex having a reversed EPR spectrum did not form although the spectral background was very noisy (receiver gain was 25–50 times that used for CuY-10). Therefore, the experiment was repeated with CuA-6. By use of a higher gain and a higher time constant than for the copper Y zeolites, the two weak high-field lines were visible in the spectrum of the hydrated sample (evacuated for 30 s). After evacuation of the sample for 5.5 h at ambient temperature, the spectrum in Figure 2 was obtained, where the magnification is 16 times that used for the CuY-10 spectrum in Figure 1C. It is clear that the simple $Cu(H_2O)_6^{2+}$ complex does not exist in this evacuated zeolite.

Copper(II) Ammine Complexes. Adding excess ammonia to dehydrated CuY-10 and CuY-32 yielded the EPR spectrum in each case that is typical[15] for the $Cu(NH_3)_4^{2+}$ complex. The $g_{\parallel}$ values varied from 2.24 to 2.27 and $A_{\parallel}$ lay in the 168–175-G range, while $g_{\perp}$ was approximately 2.04. Evacuating these samples at 373 K resulted in the appearance in the EPR spectra of reversed spectra having $g_{\parallel} = 2.00$ (135 ± 5) and

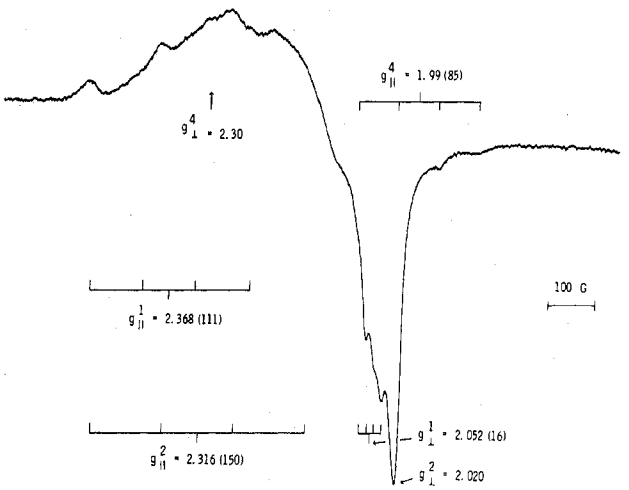

Figure 2. EPR spectrum produced by evacuating CuA-6 for 5.5 h at ambient temperature.

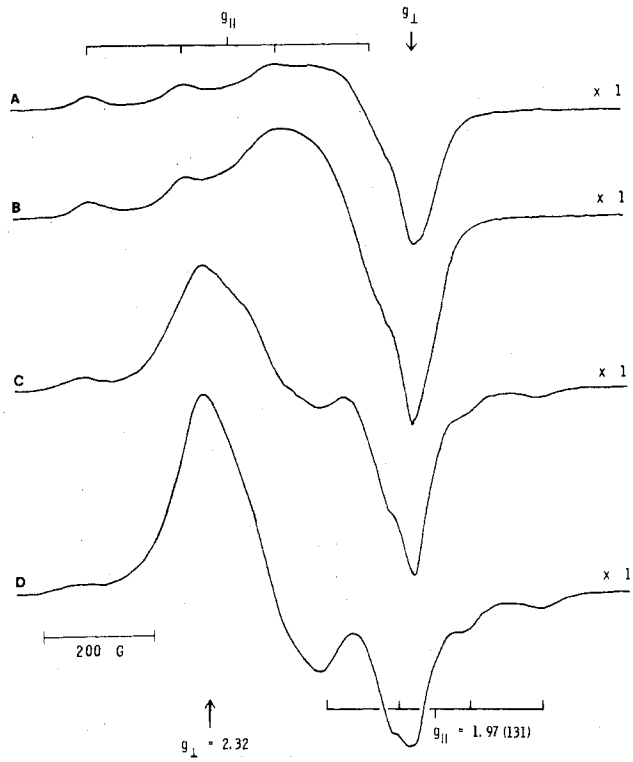

Figure 3. The EPR spectrum (A) of CuY-60 that had been reduced, equilibrated with excess NH_3, evacuated, and exposed to 20 torr of NO. Spectra B, C, and D were obtained after equilibrating at ambient temperature for 1, 25, and 42 h, respectively.

$g_{\perp} \approx 2.30$, where the latter value represents the line maximum. The reversed spectrum was always superimposed onto one or more "normal" spectra due to other Cu(II) species, in agreement with the spectra previously reported.[12]

Adding NH_3 to activated CuY-60 resulted in the superposition of the spectrum due to the tetraammine complex onto the spectrum of spin-paired Cu(II) ions, as had been observed elsewhere.[15] Therefore, a CuY-60 sample was activated, reduced, equilibrated with excess NH_3, and evacuated as described in the Experimental Section. The resultant zeolite was white and exhibited no EPR spectrum due to Cu(II). Upon addition of 20 torr of NO as an oxidant, the sample immediately became light blue and yielded the spectrum shown in Figure 3A, where $g_{\parallel} = 2.270$ (169) and $g_{\perp} = 2.036$ are attributable to the $Cu(NH_3)_4^{2+}$ complex. After equilibration of the mixture for 1, 25, and 42 h, spectra 3B, 3C, and 3D

were obtained. The high-field lines in Figures 3C and 3D are not due to the Cu^+–NO complex.[16,17] In fact, after the mixture was allowed to stand for 135 h, mass spectrometry demonstrated that the NO had been converted to N_2 and N_2O, where the corrected N_2/N_2O ratio was 1.28 ± 0.05.

A fresh portion of CuY-60 was prepared as described in the Experimental Section, and the reduced zeolite was equilibrated with 2 torr of NH_3. Upon the addition of 10 torr of O_2 at 200 K, the sample instantly became light blue and exhibited an EPR spectrum, similar to Figure 3A, characteristic of the $Cu(NH_3)_4^{2+}$ complex. Following equilibration at ambient temperature, a weak reversed spectrum was observable, but the EPR spectra quickly became dominated by the symmetrical line due to spin-paired Cu(II) ions. After the sample had equilibrated for about 185 h, analysis of the gas phase indicated that an appreciable quantity of the ammonia had been converted into nitrogen and dinitrogen oxide, where the corrected N_2/N_2O ratio was 184. There was less O_2 present than N_2O and, although a trace of water was detected in the gas phase, most of the H_2O formed would have been adsorbed by the zeolite.

Discussion

The percentages of Cu(II) in the aquo and ammine complexes that produced reversed EPR spectra were never observed to approach 100%, as judged by the intensity of the EPR lines. Therefore, a number of Cu(II) complexes were always present, and the volumetric data derived from desorption experiments would represent the average ligand (L)/Cu(II) ratio for these complexes. Thus, CuL_n complexes (with n = 0–4) could all exist in the evacuated zeolites and yield an average n in the range of 1–2.

A reversed EPR spectrum ($g_\perp > g_\parallel$) could be obtained for Cu(II) complexes having any of the following geometries: (1) compressed tetragonal octahedral (D_{4h}), (2) compressed rhombic octahedral (D_2), (3) trigonal bipyramid (D_{3h}), (4) cis-distorted octahedral (C_{2v}), and (5) linear ($D_{\infty h}$).[18] The unpaired electron in all of these configurations would be in the d_{z^2} orbital. Copper(II) ions in any of the three octahedral geometries listed would not be expected in zeolites nor would the linear configuration. Elongated octahedral and square-pyramidal complexes could be envisaged, but these would have a $d_{x^2-y^2}$ ground state and would yield normal EPR parameters. Although site I in the hexagonal prisms of Y zeolite would yield an octahedral field, it is an anhydrous site and the EPR spectrum due to Cu(II) ions in the site would not be expected to change upon dehydration; these sites are not present in zeolite A. Compressed or elongated tetrahedral complexes (D_{2d}), where the copper ion would be displaced off the trigonal axis, would not produce a d_{z^2} ground state. Therefore, from symmetry considerations case (3) is the most probable configuration attributable to the reversed EPR parameters.

It has been suggested several times that the reversed EPR spectrum is due to a $(O(2))_3CuL^{2+}$ species with a trigonal-pyramidal configuration that is referred to as a distorted tetrahedron. The resultant symmetry is C_{3v} with the L ligand on the trigonal axis. Without the L ligand and with the Cu(II) ion in the O(2) trigonal plane, the symmetry is D_{3h} and the energy term diagram has been presented.[19] As the Cu(II) ion is moved out of the plane and along the trigonal axis, the orbital energy levels change very little as the tetrahedral angle is approached, and the ground state remains a degenerate e′ state.[19,20] In the case where L (=oxygen species) approaches the fourth apex of the tetrahedron as the copper ion moves along the trigonal axis such that the O(2)–Cu–L angle changes from 90 to 109°, the energy levels rapidly approach one another and result in the t_2 (e′ = $d_{x^2-y^2}$, d_{xy} and $a_1' = d_{z^2}$ in D_{3h}) and e (e″ = d_{xz}, d_{yz} in D_{3h}) energy states expected for T_d.[20] In the situation where L is fixed in the appropriate position as the Cu(II) ion begins to move out of the plane, the resultant energy states are the same but the lower energy e″ and a_1' levels, which are close to one another, are expected to be reversed.[21] With the 3d orbitals of the divalent copper susceptible to Jahn–Teller splitting, it is expected that this cation would move off of the trigonal axis and have a non-degenerate ground state. The symmetry would approach D_{2d}, and the unpaired electron would probably be found mainly in the d_{xy} orbital, which would produce a normal EPR spectrum.

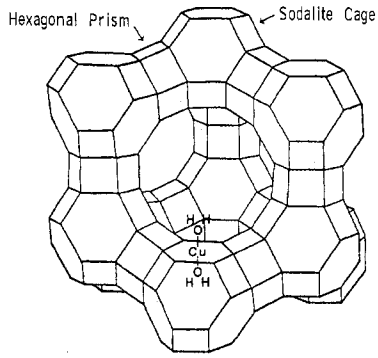

Figure 4. A representation of the Y zeolite structure showing the diaquocopper(II) cation stabilized in a 6-ring window of a sodalite cage.

The model used above has been presented elsewhere,[12,19–21] and the calculations have been thoroughly discussed.[19–21] A final point is that an a_1 ground state and a reversed EPR spectrum could be obtained if the L ligand pulled the Cu(II) ion strongly away from the three O(2) ligands and past the T_d cation position on the trigonal axis.[20,21] This would not be expected, especially with the more electrostatically charged A zeolite. As an example, the O–Co–L angle for CoA-CO was found to be 104.6°.[22]

A line drawing of the Y zeolite structure is presented in Figure 4, where every line intersection represents a Si or Al atom. The small cages are designated, and the supercage is the large central cavity. The 6-ring window has a maximum diameter of 0.26 nm but is usually considered to have an average diameter of 0.22 nm, and to enter the sodalite cage a molecule must be small enough to pass through this window. In addition, the molecule must be able to displace the Na^+ ion (in sodium Y zeolite there are 56 Na^+ ions per unit cell) that occupies the center of the window. Through dipole–cation interaction, this occurs with water and ammonia, which have kinetic diameters of 0.265 and 0.26 nm, respectively.[4] This probably does not take place with any other polar molecule because of size considerations; e.g., the kinetic diameter of CO is 0.376 nm, while that of NO is 0.317 nm. It has been found by X-ray powder diffraction techniques that in dehydrated CuY-57, the Cu(II) ions prefer site I′ in the sodalite cages.[23] The same result was found for Cu(II) faujasite, which has the same crystal structure as Y zeolite.[24] The copper(II) ion, with a diameter of about 0.14 nm, can easily fit through the 6-ring window.

The proposed model for the trigonal-bipyramidal diaquo complex in Y zeolite is given in Figure 5, where the Cu(II) ion is located in the center of the 6-ring window between sites II and II′ (designated as site IIA in ref 24). The $Cu(NH_3)_2^{2+}$–Y zeolite complex would be similar with NH_3 molecules in the axial positions. The diaquo complex in A zeolite would be the same as in the Y zeolite, but the ring oxygens would now be designated as O(3) (coordinated to the Cu(II) ion) and O(2). The diaquo and diammine complexes would form only when one ligand molecule was "trapped" in the sodalite cage during the evacuation of excess ligand. Under mild evacuation conditions, a second ligand molecule would

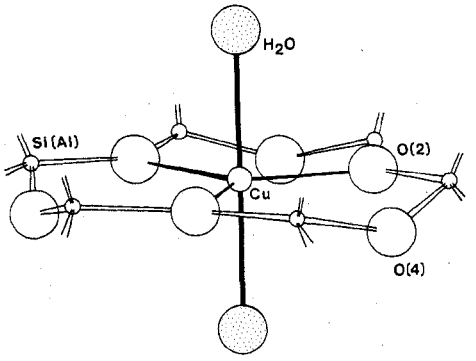

Figure 5. The model of the diaquocopper(II) complex in Y zeolite showing the trigonal symmetry. The Cu–O(2) bond distance is approximately 0.22 nm, while the Cu–O(4) distance is about 0.29 nm.[24]

coordinate to the copper in the other axial position and would protrude into the supercage (Figure 4), while evacuation at elevated temperatures would destroy the complexes (Figure 1). It is evident that the diaquo complex is less stable than is the diammine complex since the former is destroyed at 373 K while the latter is not.

The proposed pentacoordinate configuration accounts for the observation that the reversed EPR spectra are not generated during the stepwise addition of ammonia or water to the activated copper(II) zeolites but only appear during desorption or during the formation of divalent copper in situ by oxidation; the ligand molecules must already be in the sodalite cages, whose windows have become blocked by metal ions. In the addition of gaseous ligands to the activated zeolites, the Cu(II) ions migrate out of the sodalite cages and into the supercages where they form tetra- or hexacoordinated complexes faster than the ligands can migrate into the sodalite cages. The latter process is reported to be quite slow at ambient temperature.[4] It is of interest to note that in partially dehydrated copper(II) faujasite, most of the copper ions crystallographically located in the area of the 6-ring windows, including sites II and II′, were situated in the center of the windows (position IIA),[24] as proposed here for the diligated species.

Addition of NO to ammoniated highly exchanged copper(I) Y zeolite resulted in the oxidation of the copper to initially form planar $Cu(NH_3)_4^{2+}$ complexes. Since the sample had been previously evacuated, only a limited quantity of ammonia was available for complexation. As the quantity of divalent copper increased, the concentration of tetraamminecopper(II) complexes decreased while the number of diamminecopper(II) moieties increased, as shown by Figure 3. In addition, the NH_3 and NO molecules were being converted into N_2, N_2O, and H_2O, which decreased the amount of ammonia in the system. It has been previously reported that N_2O is derived from the NO molecules while the N_2 is formed by the reaction of gas-phase NO with complexed NH_3 groups.[25] The results obtained when using O_2 as the oxidant rather than NO agree with that proposal; almost all of the resultant gas phase consisted of N_2. Oxygen was observed to be a better oxidant than nitrogen monoxide, and equilibration in O_2 appeared to deplete the system of NH_3.

The g values of vertified trigonal-bipyramidal copper(II) complexes in the solid state are given in Table I.[26-30] The spectra of the polycrystalline samples were obtained at ambient temperature, but it should be noted that at 4.2 K, $g_\perp = 2.199$ and $g_\parallel = 1.998$ for $Cu(NH_3)_2Ag(SCN)_3$.[27] These five-coordinate complexes with mainly nitrogen ligands have a lower absorption band located in the $(11-13) \times 10^3$ cm^{-1} range.[18,26] This overlaps with the absorption bands noted for hydrated and dehydrated copper(II) zeolites,[8,9] and therefore the d_{z^2} and $d_{x^2-y^2}$ ground states for the trigonal Cu(II) ions and complexes in A and Y zeolites can not be differentiated by optical spectroscopy. On the other hand, distorted tetrahedral monoaquo- and monoamminecopper(II) complexes in these zeolites should exhibit absorption bands at lower wavenumbers. Since it appears that the concentrations of the latter complexes would be very low, the EPR spectra of the complexes would be expected to be obscured by the spectra of the bare Cu(II) ions and of the higher solvated complexes (parameters of the former would be similar to the latter), and the low-energy absorption bands would be of low intensity and might fall under the leading edge of the absorption envelope due to naked Cu(II) ions or to CuL_4 complexes. It has been difficult to demonstrate the existence of these bands by deconvolution techniques.[8,9]

Table I. Trigonal-Bipyramidal Copper(II) Complexes

complex[a]	$g_\perp$	$g_\parallel$	ref
$Cu(NH_3)_2Ag(SCN)_3$	2.207	2.004	26
	2.201	2.006	27
$Cu(NH_3)_2(NCS)_2$	2.278	2.058	26
[Cu(tren)NCS]SCN	2.178	2.060	26
[Cu(Me$_6$tren)Br] Br	2.182	1.956	27
[Cu(Me$_6$tren)I] I	2.226	1.895	27
$[Cu(bpy)_2I]I$	2.169	2.033	28
$[Cu(bpy)_2(tu)][ClO_4]_2$	2.165	2.022	29
$[Cu_2(tren)_2(CN)_2][BPh_4]_2$	2.134	2.006	30

[a] tren = 2,2′,2″-triaminotriethylamine, bpy = 2,2′-bipyridyl, tu = thiourea, Me$_6$tren = tris(2-dimethylaminoethyl)amine, BPh_4 = tetraphenylboron.

For a Cu(II) ion in a trigonal-bipyramidal site having a d_{z^2} ground state, the expected g values are $g_\parallel = 2.00$ and $g_\perp = 2.00 + (6k^2\lambda/\Delta E)$, where k is an orbital reduction factor, λ is the spin–orbit coupling constant (free ion value = −829 cm^{-1}), and ΔE is the energy of the d–d transition. Taking average values of 12000 cm^{-1} for ΔE and 0.76 for k for a CuN_5^{2+} complex,[26] $g_\perp$ for the $(O(2))_3Cu(NH_3)_2^{2+}$ complex is calculated to be 2.24. The maximum experimental $g_\perp$ value is somewhat higher, perhaps due to the equatorial O(2) lattice oxygens. Typically, ΔE will shift to lower energies by about 2000 cm^{-1} upon substitution of oxygen ligands for the nitrogen ligands.[31] With $\Delta E = 10000$ cm^{-1}, $g_\perp$ for the $(O(2))_3Cu(H_2O)_2^{2+}$ complex is calculated to be 2.29. Increasing the orbital reduction factor to 0.80 yielded the experimental $g_\perp$ value of 2.31. Deviations of $g_\parallel$ from 2.00 are observed in Table I and in the present results. These will not be discussed because they are minor and because possible causes of these deviations have been presented elsewhere.[27]

In general, it is found that without much difficulty Ni(II), Co(II), and Zn(II) form tetrahedral complexes that are stable in solution, as well as in the solid state. Copper(II) is observed to be tetrahedrally coordinated in only a few compounds, and in those cases mainly with soft ligands. Manganese(II) does not form stable tetrahedral complexes in aqueous solution nor with donor ligands.[32] This trend has been documented for the transition-metal ions in A zeolite,[1-3,5] with uncertainty in regard to Cu(II). It would now appear that the behavior of Cu(II) in solvated zeolites is very complicated and can result in the formation of complexes of nearly every symmetry during the various solvation, evacuation, and activation treatments.

Acknowledgment. This research was initiated at Texas A&M University with partial support by the Robert A. Welch Foundation under Grant No. A-257 and continued at Lehigh University with support from the Center for Surface and Coatings Research and partial support by the National Science Foundation.

Registry No. Cu^{2+}, 15158-11-9.

References and Notes

(1) C. L. Kovaciny, M.S. Thesis, University of Hawaii, 1973.

(2) P. E. Riley and K. Seff, *J. Phys. Chem.*, **79**, 1594 (1975).
(3) K. Seff, *Acc. Chem. Res.*, **9**, 121 (1976).
(4) The structural frameworks of the various aluminosilicate zeolites are described in detail in D. W. Breck, "Zeolite Molecular Sieves", Wiley, New York, 1974.
(5) R. Y. Yanagida, T. B. Vance, Jr., and K. Seff, *Inorg. Chem.*, **13**, 723 (1974).
(6) K. Klier and M. Rálek, *J. Phys. Chem. Solids*, **29**, 951 (1968).
(7) K. Klier, *Adv. Chem. Ser.*, **No. 101**, 480 (1971).
(8) J. Texter, D. H. Strome, R. G. Herman, and K. Klier, *J. Phys. Chem.*, **81**, 333 (1977).
(9) W. deWilde, R. A. Schoonheydt, and J. B. Uytterhoeven, *ACS Symp. Ser.*, **No. 40**, 132 (1977).
(10) R. G. Herman and D. R. Flentge, *J. Phys. Chem.*, **82**, 720 (1978).
(11) C. Naccache and Y. Ben Taarit, *Chem. Phys. Lett.*, **11**, 11 (1971).
(12) E. F. Vansant and J. H. Lunsford, *J. Phys. Chem.*, **76**, 2860 (1972).
(13) N. G. Maksimov, V. F. Anufrienko, and K. G. Ione, *Dokl. Akad. Nauk SSSR*, **212**, 142 (1973).
(14) Y.-Y. Huang and E. F. Vansant, *J. Phys. Chem.*, **77**, 663 (1973).
(15) D. R. Flentge, J. H. Lunsford, P. A. Jacobs, and J. B. Uytterhoeven, *J. Phys. Chem.*, **79**, 354 (1975).
(16) C. C. Chao and J. H. Lunsford, *J. Phys. Chem.*, **76**, 1546 (1972).
(17) R. G. Herman, *Inorg. Nucl. Chem. Lett.*, **14**, 325 (1978).
(18) B. J. Hathaway and D. E. Billing, *Coord. Chem. Rev.*, **5**, 143 (1970).
(19) K. Klier, P. J. Hutta, and R. Kellerman, *ACS Symp. Ser.*, **No. 40**, 108 (1977).
(20) R. Kellerman and K. Klier in "Surface and Defect Properties of Solids", Vol. 4, M. W. Roberts and J. M. Thomas, Ed., Billing & Sons, London, 1975, pp 1–33.
(21) P. J. Hutta, Ph.D. Dissertation, Lehigh University, Bethlehem, PA, 1974, p 40.
(22) P. E. Riley and K. Seff, *Inorg. Chem.*, **13**, 1355 (1974).
(23) P. Gallezot, Y. Ben Taarit, and B. Imelik, *J. Catal.*, **26**, 295 (1972).
(24) I. E. Maxwell and J. J. deBoer, *J. Phys. Chem.*, **79**, 1874 (1975).
(25) W. B. Williamson and J. H. Lunsford, *J. Phys. Chem.*, **80**, 2664 (1976).
(26) R. C. Slade, A. A. G. Tomlinson, B. J. Hathaway, and D. E. Billing, *J. Chem. Soc. A*, 61 (1968).
(27) R. Barbucci, A. Bencini, and D. Gatteschi, *Inorg. Chem.*, **16**, 2117 (1977).
(28) H. Elliott, B. J. Hathaway, and R. C. Slade, *J. Chem. Soc. A*, 1443 (1966).
(29) K. T. McGregor and W. E. Hatfield, *J. Chem. Soc., Dalton Trans.*, 2448 (1974).
(30) D. M. Duggan, R. G. Jungst, K. R. Mann, G. D. Stucky, and D. N. Hendrickson, *J. Am. Chem. Soc.*, **96**, 3443 (1974).
(31) B. J. Hathaway, *J. Chem. Soc., Dalton Trans.*, 1196 (1972).
(32) F. A. Cotton and G. Wilkinson, "Advanced Inorganic Chemistry", Interscience, London, 1966, p 837.

Contribution from the Chemistry Department, University of Otago, Dunedin, New Zealand

Paramagnetic Organometallic Molecules. 6.[1] Line Widths and Line Shapes in ESR Spectra of Organometallic Radicals

BARRIE M. PEAKE,* PHILIP H. RIEGER,*† BRIAN H. ROBINSON,* and JIM SIMPSON

Received September 8, 1978

The sources of line broadening and line-shape distortion in isotropic ESR spectra of organometallic radicals containing two or more equivalent nuclei have been examined in some detail. Second-order hyperfine splittings are shown to lead to asymmetric line shapes in both isotropic and frozen-solution spectra. The X-band and Q-band ESR spectra of the $C_6H_5CCo_3(CO)_9$ radical anion have been analyzed as a test of the theory. Computer simulations of the experimental isotropic spectra show that the principal line-width contribution results from incomplete averaging of anisotropies in the **g** and hyperfine tensors.

Introduction

In previous reports of the electron spin resonance (ESR) spectra of tricobalt carbon enneacarbonyl radical anions, $YCCo_3(CO)_9^-$,[2] markedly asymmetric line shapes have been noted, and a variety of explanations have been offered. In this paper, we examine in detail the factors which contribute to line shapes and line widths in the ESR spectra of organometallic radicals and radical ions. We will show that asymmetric line shapes are expected whenever the ESR spectrum has hyperfine splitting due to two or more equivalent nuclei. The theory is tested by a line-shape and line-width analysis of the ESR spectrum of the $C_6H_5CCo_3(CO)_9$ radical anion which employed computer simulation of the experimental spectra.

Theory

Isotropic ESR Spectra. Solution ESR spectra of radicals with one unpaired electron can be interpreted in terms of the spin Hamiltonian

$$H = \langle g\rangle\mu_B\vec{B}\cdot\vec{S} + \sum_i \langle A_i\rangle\vec{I}_i\cdot\vec{S} \qquad (1)$$

where $\langle g\rangle$ is the isotropic g factor, μ_B is the Bohr magneton, $\vec{B}$ is the magnetic flux density, $\langle A_i\rangle$ is the isotropic hyperfine coupling constant of the ith nucleus, and $\vec{S}$ and $\vec{I}_i$ are the electron and nuclear spin operators. If the magnetic field defines the axis of quantization (taken to be the Z axis), eq 1 can be written

$$H = \langle g\rangle\mu_B BS_Z + \sum_i \langle A_i\rangle[I_{iZ}S_Z + \tfrac{1}{2}(I_{i+}S_- + I_{i-}S_+)] \qquad (2)$$

† On leave from Brown University, Providence, R.I.

If product wave functions $|m_S, m_1, m_2, \ldots\rangle$ are used as a basis set, eq 2 can be used to predict ESR lines, to second order in perturbation theory, at field positions

$$B = B_0 - \sum_i \langle a_i\rangle m_i - \sum_i \frac{\langle a_i\rangle^2}{2B}[I_i(I_i+1) - m_i^2] \qquad (3)$$

where I_i and m_i are the nuclear spin and Z-component quantum number of the ith nucleus, $\langle a_i\rangle = \langle A_i\rangle/\langle g\rangle\mu_B$ is the hyperfine coupling constant in magnetic flux density units, and $B_0 = h\nu_0/\langle g\rangle\mu_B$ is the center field when the microwave frequency is ν_0.

If the nuclear spins are completely equivalent, that is equivalent both instantaneously and over a time average, then it is appropriate to describe the spin system in the "coupled representation" with the quantum numbers J and M of the total nuclear spin angular-momentum operators $\vec{J} = \sum\vec{I}_i$.[3,4] In the coupled representation, the spin Hamiltonian is

$$H = \langle g\rangle\mu_B BS_Z + \langle A\rangle[I_ZS_Z + \tfrac{1}{2}(J_+S_- + J_-S_+)] \qquad (4)$$

and the zero-order basis set of nuclear spin wave functions consists of linear combinations of the product wave functions which are eigenfunctions of J^2, J_Z, and the appropriate symmetry operators.

In the case of three equivalent spin $^7/_2$ nuclei, 11 values of J are found, ranging from $J = {}^1/_2$ to $J = {}^{21}/_2$. The 22 basis functions corresponding to $J = {}^{21}/_2$ are of the symmetry type A_1 and include all possible values of M ($\pm{}^{21}/_2, \pm{}^{19}/_2, \ldots, \pm{}^1/_2$). The four basis functions corresponding to $J = {}^1/_2$ are of symmetry type E and include $M = \pm{}^1/_2$. The symmetries of the other basis functions for this case are given in Table I.

0020-1669/79/1318-1000$01.00/0 © 1979 American Chemical Society